ELSEVIER

Solid State Ionics 100 (1997) 45–52

SOLID STATE IONICS

Transport properties of $BaCe_{0.95}Y_{0.05}O_{3-\alpha}$ mixed conductors for hydrogen separation

J. Guan[a], S.E. Dorris[a], U. Balachandran[a,*], M. Liu[b]

[a]*Energy Technology Division, Argonne National Laboratory, Argonne, IL 60439, USA*
[b]*School of Materials Science and Engineering, Georgia Institute of Technology, Atlanta, GA 30332, USA*

Received 14 April 1997; accepted 28 April 1997

Abstract

We have characterized the transport properties of a mixed ionic–electronic conductor, $BaCe_{0.95}Y_{0.05}O_{3-\alpha}$ (BCY), by using impedance spectroscopy and open-cell voltage measurements. Such mixed conductors have many applications, including hydrogen separation. Results indicate that in an oxygen/water vapor atmosphere, proton conduction is dominant at low temperatures (500 to 600°C) while oxygen ion conduction dominates at higher temperatures (700 to 800°C). In a hydrogen/water vapor atmosphere, however, proton conduction dominates over the entire temperature range studied (500 to 800°C). The proton conductivity of BCY ranges from 1.9×10^{-3} Ω^{-1} cm^{-1} at 800°C in an oxygen/water vapor atmosphere to 1.27×10^{-2} Ω^{-1} cm^{-1} in a hydrogen/water vapor atmosphere. Compared to protonic conductivity ($\approx 7.2 \times 10^{-3}$ Ω^{-1} cm^{-1}), electronic conductivity in a H_2/H_2O atmosphere is relatively low ($\approx 2.1 \times 10^{-3}$ Ω^{-1} cm^{-1}) at 700°C and must be enhanced in order to improve the rate of gas permeation when BCY is used as a membrane for gas separation.

Keywords: H_2 Separation; Proton conductor; Mixed conductor; $BaCeO_3$; Transference number

1. Introduction

Mixed conductors have found many applications, including solid oxide fuel cells, solid-state gas sensors, and membranes for gas separation [1–7]. Perovskite-type oxides are extensively studied due to their high ambipolar conductivities. These materials are usually electronic and oxygen ionic conductors that can be used in oxygen separation, oxygen sensors, and solid oxide fuel cells. In a hydrogen-free atmosphere, the ionic current is carried only by oxygen ions but protonic conduction is observed in hydrogen-containing atmospheres. This was first discovered by Iwahara et al. in $SrCeO_3$ materials [1], and $BaCeO_3$ compounds were later extensively studied due to their higher conductivities [8–11]. It is generally agreed that barium cerate electrolytes exhibit both oxygen ion and proton conduction; the oxygen ion and proton transference numbers depend on temperature and atmosphere. In $BaCeO_3$ compounds, a gradual transition from proton to oxygen ion transport occurs with increasing temperature [9,10,12,13]. Bonanos et al. and Knight related this transition phenomenon to structure properties and claimed that phase transformation might be responsible for the transition [14–16].

In hydrogen/oxygen solid oxide fuel cells, it is the

*Corresponding author: Tel: +1 630 252 4250; fax: +1 630 252 3604; e-mail: u_balachandran@qmgate.anl.gov

0167-2738/97/$17.00
PII S0167-2738(97)00320-2

total ionic transference number, not the oxygen ion or proton transference number, that determines fuel cell performance. For gas separation, however, the preference is for only one gas species to transport through the ceramic membrane. For H_2 separation from oxygen-free gas mixtures, it is reasonable to neglect oxygen transport. But in an oxygen-containing atmosphere, oxygen conduction must be taken into account because oxygen ion transport may be inevitable in these perovskite-type materials. In gas mixtures from which hydrogen is to be separated, such as recycled gases and synthesis gases, water vapor is present as well and may contribute to oxygen ion conduction.

In this study, transport properties are characterized by impedance spectroscopy and open-cell voltage (OCV) measurements on concentration cells of oxygen, water vapor, and hydrogen [17–22].

2. Experimental

2.1. Sample preparation

We synthesized 5% Y-doped $BaCeO_3$ (BCY) via solid-state reactions. $BaCO_3$ (Mallinckrodt), CeO_2 (Trona Chemicals), and Y_2O_3 (Trona Chemicals) with the desired stoichiometric ratio were ball-milled for at least 24 h and then calcined for 12 h at 1000°C in air. The powders were then ground and recalcined in air for 10 h at 1200°C. The resulting powders, confirmed by X-ray diffraction to be of perovskite structure (Fig. 1), were then uniaxially pressed into pellets with a 2.2 cm diameter die under a pressure of 100 MPa. The pellets were then sintered in air for 10 h at 1550°C. Relative densities of the sintered pellets were ≈92%. Crack-free pellets were polished on two sides and Pt mesh (#80) was

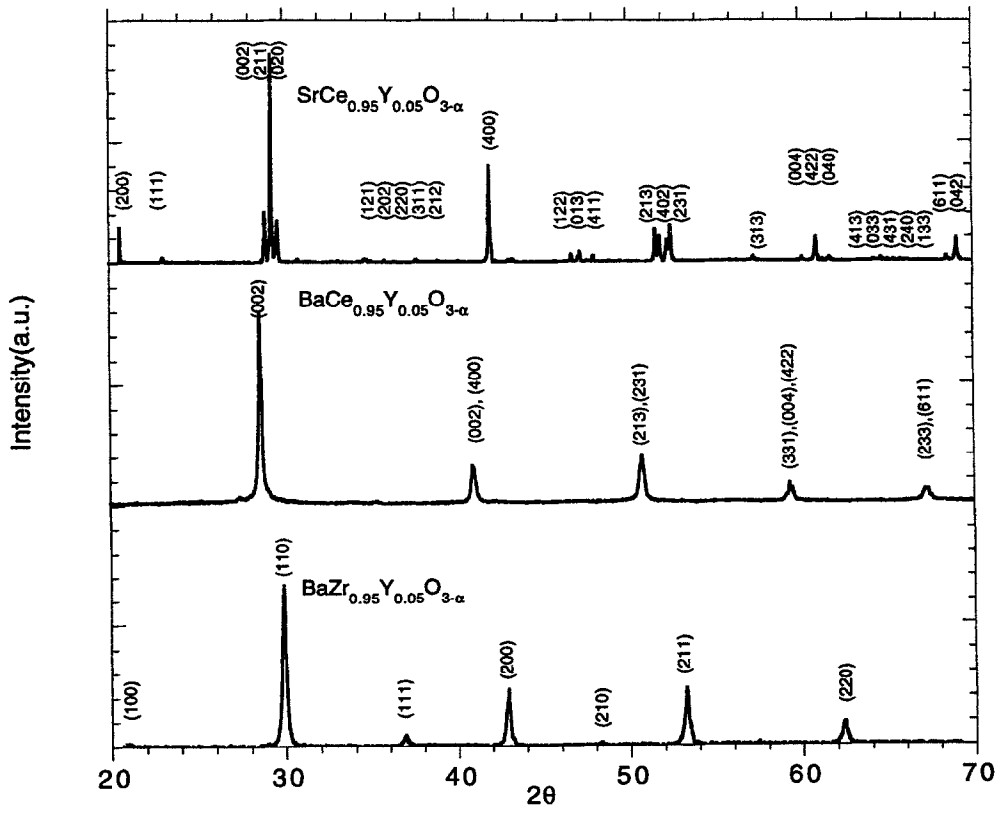

Fig. 1. X-ray diffraction patterns for Y-doped $SrCeO_3$, $BaCeO_3$ and $BaZrO_3$.

attached to the polished surfaces with Ag paste (Heraeus C1000), which was then dried at 150°C for 2 h and fired at 850°C for 30 min in air. The resulting pellets were sealed onto the end of an Al_2O_3 tube by a glass sealant, ANL Mat43 ($SrO:La_2O_3:Al_2O_3:B_2O_3:SiO_2$ = 41.76:3.74:16.27:27.01:11.23) [23]. The glass powders were mixed with ethylene glycol as binder and isopropyl alcohol as a dispersant. The sealed structure was first air-dried, then heated slowly (20°C per h ramp and 5-h dwell at 350°C) to burn out the binder, and finally devitrified at 780°C.

2.2. Impedance spectroscopy

Impedance spectra of cells with Pt/Ag electrodes and BCY electrolyte were measured with an impedance analyzer (HP4192A LF) in the frequency range of 13 MHz to 5 Hz. Water vapor was obtained by bubbling the selected gas through deionized water at either room temperature (22–23°C) or at 40°C in a constant-temperature water bath (PolyScience, 7305). In the latter case, tubes circulating with 40°C water were wrapped around the gas flow tube between the bubbling bottle to the furnace to prevent water vapor condensation. Water vapor pressure was measured by an instant digital hygrometer (Fisher Scientific) and the measured values are consistent with the standard data [24].

2.3. OCV measurements with concentration cells

For a concentration cell exposed to different gases (gases I and II), OCV can be expressed as [20]:

$$V_{oc} = -\frac{1}{F}\sum_k \int_{\mathrm{I}}^{\mathrm{II}} \frac{t_k}{z_k}\, \mathrm{d}\mu_k^* \tag{1}$$

where the chemical potential of species k is

$$\mu_k^* = \tilde{\mu}_k + z_k\tilde{\mu}_e. \tag{2}$$

$\tilde{\mu}_k$ is the electrochemical potential of defect k, $\tilde{\mu}_e$ is the electrochemical potential of electrons, t_k is transference number for defect k, and z_k is the charge number of defect k.

In a concentration cell containing oxygen and water vapor, the electrode reactions include

$$\tfrac{1}{2}\,O_2 + 2e' \Leftrightarrow O^{2-}, \tag{3}$$

$$H_2O(g) \Leftrightarrow 2H^+ + \tfrac{1}{2}\,O_2(g) + 2e'. \tag{4}$$

Integrating Eq. (1) over the thickness of the electrolyte, we have

$$V_{oc} = \frac{RT}{4F}\left[t_{ion}\ln\left(\frac{p_{O_2}^{\mathrm{II}}}{p_{O_2}^{\mathrm{I}}}\right) - 2t_H\ln\left(\frac{p_{H_2O}^{\mathrm{II}}}{p_{H_2O}^{\mathrm{I}}}\right)\right] \tag{5}$$

where

$$t_{ion} = t_H + t_O. \tag{6}$$

When the partial pressure of water vapor is kept constant while an oxygen concentration gradient is created between gases I and II, the OCV measurement can give the total ionic transference numbers, t_{ion}, from Eq. (5). When the oxygen concentration gradient across the cell is kept constant while the water vapor partial pressure on one side of the cell is changed to create a water vapor concentration gradient, the OCV will change due to the effects of water vapor gradients. Solving these V_{oc} expressions will give the transference numbers of oxygen ions (t_O), protons (t_H), and electrons (t_e).

In a concentration cell containing hydrogen and water vapor, the electrode reactions include:

$$H_2(g) \Leftrightarrow 2H^+ + 2e', \tag{7}$$

$$H_2O(g) + 2e' \Leftrightarrow H_2(g) + O^{2-}. \tag{8}$$

Integrating Eq. (1) over the thickness of the electrolyte, we have

$$V_{oc} = \frac{RT}{2F}\left[-t_{ion}\ln\left(\frac{p_{H_2}^{\mathrm{II}}}{p_{H_2}^{\mathrm{I}}}\right) + t_O\ln\left(\frac{p_{H_2O}^{\mathrm{II}}}{p_{H_2O}^{\mathrm{I}}}\right)\right]. \tag{9}$$

A procedure like that described above can be used to determine transference numbers in this H_2/H_2O atmosphere.

In OCV measurements, BCY pellets were used as the electrolyte for concentration cells, as shown in Fig. 2. Gases I and II were fed to both sides of the cell through the gas inlets, which were very close to the sample being tested. Gas flow rates were adjusted to $\approx$100 cm^3 (STP)/min.

The OCVs of the concentration cells stabilized within several hours. At lower temperatures, e.g.,

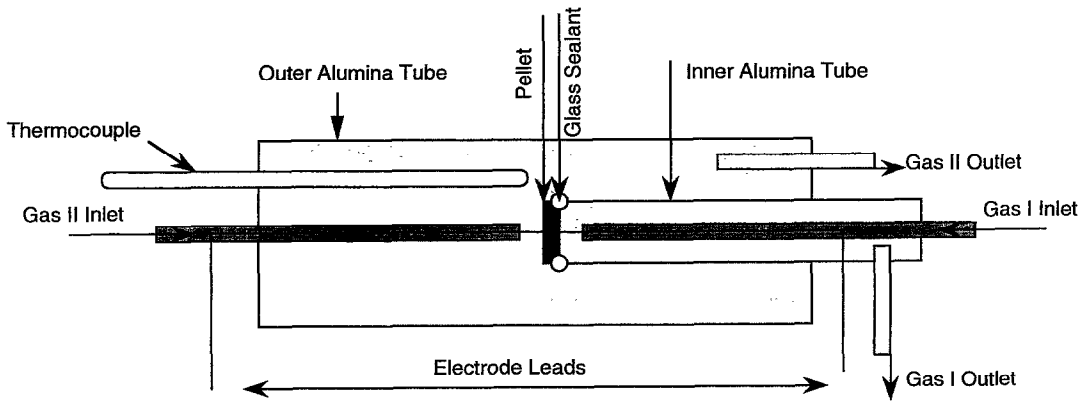

Fig. 2. Schematic illustration of testing setup.

500°C, sluggish reaction kinetics on the surface required longer equilibration times (up to 15–24 h) to stabilize the OCV.

3. Results and discussion

3.1. Total conductivity in different atmospheres

Fig. 3 shows the total conductivities of BCY pellets in different atmospheres as determined by impedance spectroscopy. Total conductivity of 5% Y-doped $BaCeO_3$ was low in pure argon even at high temperatures (≥600°C), but increased slightly with the addition of ≈2% water vapor. At low temperatures (≈550°C), total conductivity was low but increased significantly upon adding ≈2% water vapor. In pure oxygen, the total conductivity of BCY was found to be much higher than that in pure argon, but the effect of water vapor depended on temperature. At low temperatures, addition of water vapor increased the total conductivity, but at high temperatures, total conductivity decreased slightly when water vapor was added.

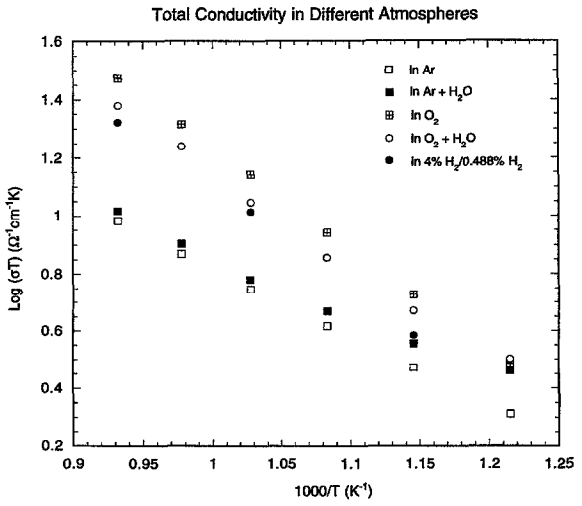

Fig. 3. Total conductivity measured in different atmospheres.

Also shown in Fig. 3 is total conductivity determined from impedance spectra of a hydrogen/water vapor concentration cell under open-cell conditions. Total conductivity increased from $4.37\times10^{-3}\ \Omega^{-1}\,cm^{-1}$ at 600°C to $1.99\times10^{-2}\ \Omega^{-1}\,cm^{-1}$ at 800°C.

3.2. Transference number

3.2.1. In oxygen-containing atmospheres

Transference numbers were determined by using the following concentration cells:

$$\text{II}, O_2 + 2.81\%H_2O, \text{Pt} \mid \text{BCY} \mid \text{Pt}, N_2 + 8\%O_2 + 2.81\%H_2O, \text{I} \quad \text{(cell 1)}.$$

$$\text{II}, O_2 + 7.38\%H_2O, \text{Pt} \mid \text{BCY} \mid \text{Pt}, N_2 + 8\%O_2 + 2.64\%H_2O, \text{I} \quad \text{(cell 2)}.$$

$$\text{II}, N_2 + 8\%O_2 + 7.38\%H_2O, \text{Pt} \mid \text{BCY} \mid \text{Pt}, O_2 + 2.81\%H_2O, \text{I} \quad \text{(cell 3)}.$$

As can be seen from Table 1, the measured OCVs of cell 1 decrease as temperature increases, indicating that the electronic transference numbers increase with temperature. When the partial pressures of water vapor were changed to the level in cell 2 while oxygen partial pressure were kept the same as in cell 1, the observed OCVs of cell 2 were quite different than those of cell 1. First, the OCVs were lower than those of cell 1 at each temperature. Second, the OCVs increased with temperature, unlike those in cell 1. Because the partial pressures of oxygen across the two cells are the same, the only possible reason is the difference in partial pressure of water vapor across these two cells. From Eq. (5), it is clear that the OCVs of cell 2 will be lower than those of cell 1 if the proton transference numbers are not zero because the water vapor gradient partially offsets the EMF arising from the oxygen gradient because of the difference in polarity. When the oxygen gradient across the cell was reversed to that of cell 3, the OCVs changed sign. When the oxygen and water vapor gradients had the same polarity (as in cell 3), higher OCVs resulted, as indicated in Table 1.

Shown in Fig. 4 are the total ionic, oxygen ion, proton, and electronic transference numbers of the mixed conductor calculated from the OCV data for cells 1 and 2. Similar results were obtained with the OCV data from cells 1 and 3. Total ionic transference number decreases as temperature increases, while the electronic transference number increases. Protons dominate ionic conduction at low temperatures (500 to 600°C), while oxygen ions dominate ionic conduction at high temperatures (700 to 800°C).

3.2.2. *In hydrogen-containing atmospheres*

Transference numbers in hydrogen/water vapor atmospheres were measured by using the following three cells:

$$\text{II}, N_2 + 4\%H_2 + 2.64\%H_2O, \text{Pt} \mid \text{BCY} \mid \text{Pt}, N_2 + 0.488\%H_2 + 2.64\%H_2O, \text{I} \quad \text{(cell 4)}.$$

$$\text{II}, N_2 + 4\%H_2 + 7.38\%H_2O, \text{Pt} \mid \text{BCY} \mid \text{Pt}, N_2 + 0.488\%H_2 + 2.64\%H_2O, \text{I} \quad \text{(cell 5)}.$$

Table 1
OCV(II–I) data for oxygen/water vapor concentration cells 1, 2, and 3

Temperature	OCV (mV)		
(°C)	Cell 1	Cell 2	Cell 3
500	32.0	14.8	−48.2
600	28.0	19.9	−36.8
700	27.2	22.1	−31.3
800	26.4	22.3	−29.7

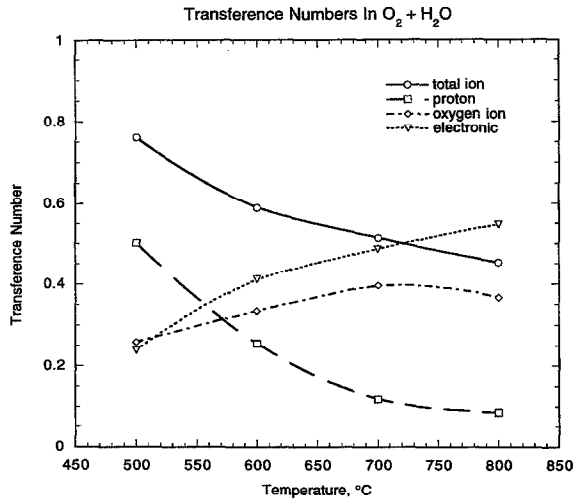

Fig. 4. Transference numbers determined in O_2/H_2O concentration cells 1 and 2.

$$\text{II}, N_2 + 0.488\%H_2 + 7.38\%H_2O, \text{Pt} \mid \text{BCY} \mid \text{Pt}, N_2 + 4\%H_2 + 2.64\%H_2O, \text{I} \quad \text{(cell 6)}.$$

The observed OCVs are listed in Table 2, while the transference numbers calculated from the OCV measurements are presented in Fig. 5. The total ionic transference number in hydrogen/water vapor en-

Table 2
OCV(II–I) data for hydrogen/water vapor concentration cells 4, 5, and 6

Temperature	OCV (mV)		
(°C)	Cell 4	Cell 5	Cell 6
500	−63.13	−62.01	64.02
600	−66.43	−64.48	68.14
700	−70.55	−65.17	75.57
800	−76.39	−69.11	83.26

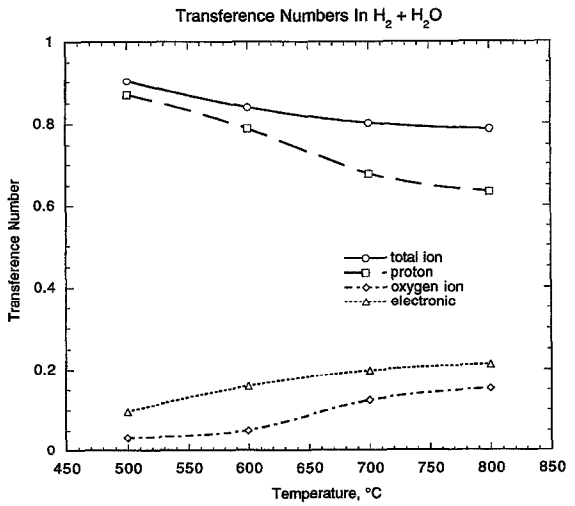

Fig. 5. Transference numbers determined in H_2/H_2O concentration cells 4 and 5.

vironments decreases from 0.90 to 0.79 when temperature increases from 500 to 800°C. Compared to those in an oxygen/water vapor atmosphere, the ionic transference number is higher in the hydrogen/water vapor atmospheres. Electronic transference numbers, however, are much lower ($t_e \approx 0.21$ at 800°C) in hydrogen/water vapor atmospheres. Proton transference numbers decrease from 0.87 to 0.63 while oxygen ion transference numbers increase from 0.03 to 0.15 as temperature increases from 500 to 800°C. Clearly, protons dominate ionic conduction over the entire range of temperatures tested. These results differ from those of Bonanos et al. [14], who show that oxygen ions dominate ionic conduction in Gd-doped $BaCeO_3$ at high temperature, even in hydrogen/water vapor atmospheres.

For a given total conductivity, ambipolar diffusion flux density reaches its maximum when the ionic transference number (oxygen ion or proton) equals the electronic transference number [7,25]. The relatively low electronic transference numbers for this material suggest that electronic transport is insufficient in the hydrogen/water vapor environments to obtain maximum H_2 flux density. To improve electronic transport, a second phase with high electronic conduction or proper doping is needed.

3.3. Partial conductivities of charged species

3.3.1. In oxygen-containing atmospheres

The conductivities of the mobile defects are calculated from

$$\sigma_i = \sigma_{total} \times t_i \,. \tag{10}$$

The results are shown in Fig. 6. Total ion, oxygen ion, and electronic conductivities increase dramatically with temperature. But proton conductivities increase slightly from 1.38×10^{-3} $\Omega^{-1}\,cm^{-1}$ to 1.93×10^{-3} $\Omega^{-1}\,cm^{-1}$ when the testing temperature increases from 600 to 800°C. These results are in agreement with those of Bonanos, Taniguchi et al., and Iwahara et al. [9,10,12,13].

3.3.2. In hydrogen-containing atmospheres

As shown in Fig. 7, all conductivities increase with increase of temperature in hydrogen/water vapor atmospheres. Unlike the slight increase in proton conductivity that was observed in the oxygen/water vapor containing atmosphere, proton conductivities increased dramatically from 3.47×10^{-3} $\Omega^{-1}\,cm^{-1}$ to 1.27×10^{-2} $\Omega^{-1}\,cm^{-1}$ when temperature increased from 600 to 800°C. It must be mentioned, however, that oxygen ion conduction

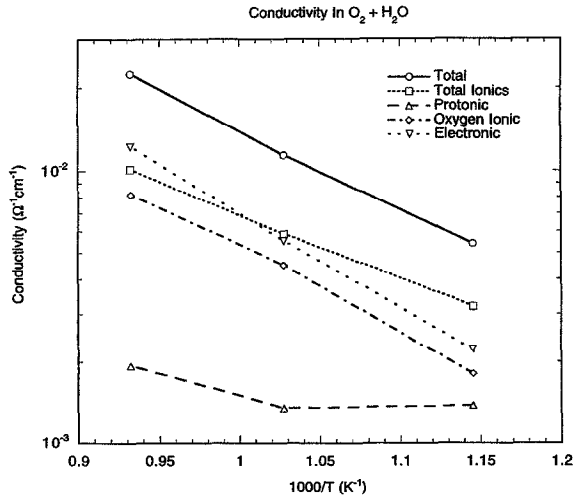

Fig. 6. Conductivity of 5% Y-doped $BaCeO_3$ in O_2/H_2O atmosphere.

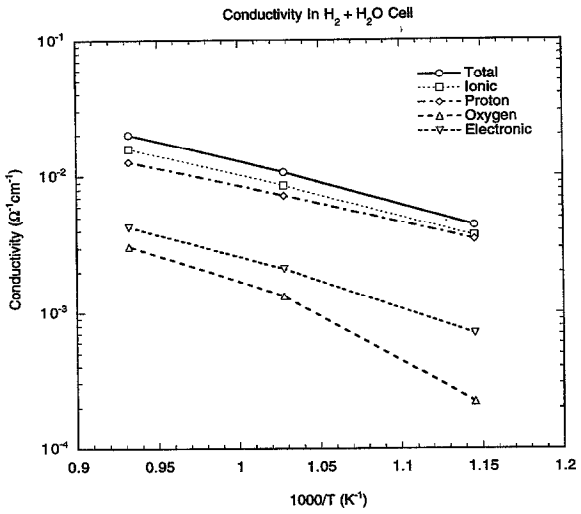

Fig. 7. Conductivity of 5% Y-doped $BaCeO_3$ in H_2/H_2O atmosphere.

remained measurable ($\approx 3\times10^{-3}$ $\Omega^{-1}\,cm^{-1}$ at 800°C) even in the hydrogen-containing atmosphere due to the presence of water vapor. This suggests that the selectivity of BCY for hydrogen separation would be improved by drying the gas mixture.

4. Conclusions

Using impedance spectroscopy and open cell voltage (OCV) measurements, we characterized the transport properties of several concentration cells based on 5% Y-doped $BaCeO_3$ (BCY). Proton conduction has been observed in this material in hydrogen/containing atmospheres. Proton and oxygen ion transference numbers were calculated from the measured OCVs. In an oxygen/water vapor atmosphere, protons dominate ionic conduction at low temperatures (500–600°C), while oxygen ions dominate at higher temperatures (700–800°C). In a hydrogen/water vapor atmosphere, proton conduction dominates over the entire range of temperature (500–800°C). The electronic conductivity of BCY in a hydrogen/water vapor atmosphere was relatively low ($\approx 2.11\times10^{-3}$ $\Omega^{-1}\,cm^{-1}$), compared to the protonic conductivity ($\approx 7.22\times10^{-3}$ $\Omega^{-1}\,cm^{-1}$) at 700°C. To optimize the properties of BCY for hydrogen separation and maximize the gas flux, electronic conductivity should be increased.

Acknowledgements

The authors thank Dr. T. Kueper of Argonne's Chemical Technology Division for supplying glass sealant. This work was supported by the U.S. Department of Energy, Federal Energy Technology Center, under Contract W-31-109-Eng-38.

References

[1] H. Iwahara, T. Esaka, H. Uchida, N. Maeda, Solid State Ionics 3/4 (1981) 359.
[2] T. Yajima, H. Suzuki, T. Yogo, H. Iwahara, Solid State Ionics 51 (1992) 101.
[3] H. Iwahara, Solid State Ionics 77 (1995) 289.
[4] N. Miura, N. Yamazoe, Solid State Ionics 53–56 (1992) 975.
[5] K. Kreuer, Chem. Mater. 8 (1996) 610.
[6] S.E. Dorris, U. Balachandran, First Joint Power and Fuel System Contractors' Conference, Pittsburgh, PA, July 9–11, 1996.
[7] M. Liu, in: Proceedings of the 1st International Symposium on Ionic and Mixed Conducting Ceramics, T.A. Ramanarayanan, H.L Tuller (Eds.), The Electrochemical Society, Pennington, NJ, 1991, p. 95.
[8] J.F. Liu, A.S. Nowick, Mater. Res. Soc. Symp. Proc., Solid State Ionics II 210 (1991) 673.
[9] N. Bonanos, Solid State Ionics 53–56 (1992) 967.
[10] N. Taniguchi, K. Hatoh, J. Niikura, T. Gamo, Solid State Ionics 53–56 (1992) 998.
[11] D.A. Steveson, N. Jiang, R.M. Buchanan, F.E.G. Henn, Solid State Ionics 62 (1993) 279.
[12] H. Iwahara, T. Yajima, H. Uchida, Solid State Ionics 70/71 (1994) 267.
[13] H. Iwahara, T. Mori, T. Hibino, Solid State Ionics 79 (1995) 177.
[14] N. Bonanos, K.S. Knight, B. Ellis, Solid State Ionics 79 (1995) 161.
[15] K.S. Knight, Mater. Res. Bull. 30 (1995) 347.
[16] K.S. Knight, Solid State Ionics 74 (1994) 109.
[17] H. Richert, Electrochemistry of Solids, Springer-Verlag, Berlin, 1982.
[18] D.P. Sutija, T. Norby, P. Bjornbom, Solid State Ionics 77 (1995) 167.
[19] T. Norby, Solid State Ionics 28–30 (1988) 1586.
[20] L. Heyne, in: S. Geller (Ed.), Solid Electrolytes, Springer-Verlag, Berlin, 1977, p. 169.
[21] M. Liu, H. Hu, J. Electrochem. Soc. 143 (1996) L109.

[22] N. Bonanos, B. Ellis, K.S. Knight, M.N. Mahmood, Solid State Ionics 35 (1989) 179.
[23] K.L. Ley, M. Krumplet, R. Kumar, J.H. Meiser, I. Bloom, J. Mater. Res. 11 (1996) 1489.
[24] D.R. Lide, Handbook of Chemistry and Physics, 75th ed., CRC Press, Boca Raton, FL, 1994.
[25] T.A. Ramanarayanan, S. Ling, M.P. Anderson, in: T.A. Ramanarayanan, H.L. Tuller (Eds.), Proceedings of the 1st International Symposium on Ionic and Mixed Conducting Ceramics, The Electrochemical Society, Pennington, NJ, 1991, p. 110.